

PAPER • OPEN ACCESS

## Investigations on Microstructure and Corrosion behavior of Superalloy 686 weldments by Electrochemical Corrosion Technique

To cite this article: B Arulmurugan and M Manikandan 2018 *IOP Conf. Ser.: Mater. Sci. Eng.* **310** 012071

View the [article online](#) for updates and enhancements.



**IOP | ebooks™**

Bringing you innovative digital publishing with leading voices to create your essential collection of books in STEM research.

Start exploring the collection - download the first chapter of every title for free.

# Investigations on Microstructure and Corrosion behavior of Superalloy 686 weldments by Electrochemical Corrosion Technique

B Arulmurugan <sup>1</sup> and M Manikandan <sup>2\*</sup>

<sup>1</sup> Assistant Professor, KPR Institute of Engineering & Technology, Coimbatore, India & Research Scholar, School of Mechanical Engineering, VIT University, Vellore, India

<sup>2</sup> Assistant Professor, School of Mechanical Engineering, VIT University, Vellore, India

E-mail: [enggarul@gmail.com](mailto:enggarul@gmail.com)

\*[mano.manikandan@gmail.com](mailto:mano.manikandan@gmail.com)

**Abstract.** In the present study, microstructure and the corrosion behavior of Nickel based superalloy 686 and its weld joints has been investigated by synthetic sea water environment. The weldments were fabricated by Gas Tungsten Arc Welding (GTAW) and Pulsed Current Gas Tungsten Arc Welding (PCGTAW) techniques with autogenous mode and three different filler wires (ERNiCrMo-4, ERNiCrMo-10 and ERNiCrMo-14). Microstructure and Scanning electron microscope examination was carried out to evaluate the structural changes in the fusion zones of different weldments. Energy Dispersive X-ray Spectroscopy (EDS) analysis was carried out to evaluate the microsegregation of alloying elements in the different weld joints. Potentiodynamic polarization study was experimented on the base metal and weld joints in the synthetic sea water environment to evaluate the corrosion rate. Tafel's interpolation technique was used to obtain the corrosion rate. The microstructure examination revealed that the fine equiaxed dendrites were observed in the pulsed current mode. EDS analysis shows the absence of microsegregation in the current pulsing technique. The corrosion rates of weldments are compared with the base metal. The results show that the fine microstructure with the absence of microsegregation in the PCGTAW weldments shows improved corrosion resistance compared to the GTAW. Autogenous PCGTAW shows higher corrosion resistance irrespective of all weldments employed in the present study.

**Keywords:** Alloy 686, Gas Tungsten Arc Welding, Pulsed Current Gas Tungsten Arc Welding, Potentiodynamic polarization, Corrosion rate

## 1. Introduction

Marine corrosion is a growing issue which leads to losses in material, energy and also money along with it burden. The corrosion in weldments of marine environment materials is commonly due to high chlorides, oxygen, biological activities, pollution, temperature, salinity and velocity of seawater [1]. These elements cause localized corrosion by means of pitting, crevice, galvanic, stress corrosion cracking (SCC) and intergranular corrosion, which don't occur uniformly throughout the metal surface.

In marine environments, the sea salt deposited on the metal/weldment surface which causes pitting corrosion along with rust formation. The galvanic and crevice corrosion are the most significant corrosion problem compared to others. This corrosion formed on the material surface due to the low resistivity of the water [2]. So protection and controlling of corrosion is the biggest challenge for materials engineer. This can be effectively achieved by selecting an appropriate material for those applications to overcome the localized corrosion. Generally, the material which possesses more Pitting Resistance Equivalent Number (PREN) value will be good for the highly corrosive environment [3]. The corrosion rate and pitting potential of the materials in seawater environment are significantly influenced by the addition of alloying elements Ni, Cr & Mo in the matrix [4]. The outstanding



corrosion resistance of nickel alloys has been set to superior use in sea water environment for many years.

In the present an attempt has been made to study the corrosion behavior of 21st century Nickel superalloy 686 and its weldments. It is a solid solution strengthened superalloy derived from Ni-Cr-Mo ternary system. The presence of combination of high Cr-Mo-W & low carbon content provides excellent resistance against seawater environments [3]. Nickel has the capability to dissolve all alloying elements and to maintain them in a single solution strengthen austenite in its matrix. Chromium in that combination is preventing oxidization by forming a stable oxide film, Mo is protecting reduction as well as pitting corrosion and the presence of tungsten is also focusing on pitting corrosion. The effect of the addition of alloying elements like Cr & Mo was explained by Hayes et al. [5] The authors reported that chromium plays a predominant role in preserving the passivity of the alloy, while molybdenum performs to stabilize the passive film. Some of the other Ni-based alloy's corrosion behavior is listed below.

Rabek and Crook [6] investigated the corrosion behavior of alloy C22 under different chemical environments by considering solution composition, temperature, and redox potential. Craig and co-worker [7] performed potentiometric study of the Corrosion of Ni-Resist in Sea Water environment and they reported that general corrosion rate of Ni-Resist increases with velocity in aerated seawater and remain constant in deaerated seawater. In general, Ni based superalloy provides excellent corrosion resistance, Alloy 686 is the best material to use in marine industries because it has the highest Pitting Resistance Equivalency Number PREN value of 51, which shows the superior quality in corrosion resistance, when compared with other alloys in the Ni-Cr-Mo ternary system. This alloy combination is enormously supporting in handling mixed acids, severe chloride surroundings in the range of 100000 to 200000 ppm and another defensive parameter is to handle the acids with a PH level of 1 or even less. [8]

The corrosion defensive property of solid solution strengthening alloys is lower than the equivalent of the wrought alloy. The reason is due to; during solidification, the fusion zone contains interdendritic secondary brittle phases and gradients of concentration because of redistribution of solute. These interdendritic phases and concentration gradients can always direct to speed up corrosion locally [4]. So the improvement in technology is essential to diminish the formation of secondary phases in the fusion of weldments during the solidification to improve corrosion resistance. It can be achieved by two methods; one is by using high density welding processes like Laser beam and Electron beam welding. For example Guangyi et al. [9] investigated the microsegregation in weldment of alloy C 276 which were fabricated by pulsed laser beam welding and found out the diminutive amount of secondary phases in the fusion zone. Manikandan et al. [10] examined the alloy C-276 by continuous Nd:YAG laser welding and reported that laser welding shows diminish microsegregation compared to other arc welding process. Radhakrishna et al.[11] evaluated fusion zone microstructure of Inconel 718 alloy using two different welding process like GTA and EB, and come to a conclusion that EB welding results in reducing the microsegregation in the interdendritic region than GTA. Even though high beam energy processes provide good results than conventional procedures, they were not economical.

The second method is using the conventional TIG welding process to suppress the effect of microsegregation by current pulsing technique. Janaki Ram et al.[12] exploited the square pulsing of welding current & reported that there is a reduced interconnectivity of Laves network and segregation of Nb, which results in improved stress rupture properties. Manikandan et al. [13-14] are also highlight the significance of pulsed current welding technique during their investigation of Hastelloy C- 276 similar and dissimilar welding. Arulmurugan and Manikandan [15] developed a welding technique using GTAW and PCGTAW to reduce the microsegregation of alloying elements to improve the metallurgical and mechanical properties of the weld joints. Authors concluded that pulsed current shows reduced microsegregation with improved mechanical properties compared to GTAW technique. There is no published literature on corrosion of weldments produced in superalloy 686 by GTAW and

PCGTAW. In their continuation of their previous work, investigates the corrosion behavior of alloy 686.

In this study, the corrosion behaviors of alloy 686 weldments were evaluated by Potentiodynamic polarization method in an artificial seawater environment. Polarization studies on different materials addressed by many researchers and the authors suggested that this approach is faster than compared to classical weight loss estimation method [16-18]. This test will provide unique information about, corrosion rate. The objective of this research is to measure the corrosion rate of the alloy 686 eight different welded samples and to compare them with base metal corrosion rate and identify the optimum weld method to be used in high aggressive sea water environment.

**2. Experimental procedure**

**2.1 Candidate materials**

Alloy 686 was procured in the form of 3 mm thick sheet. Weld coupons were extracted in the dimension of 130 mm X 55 mm X 3 mm by using wire cut electrical discharge machine (EDM). The corrosion samples were extracted from the welded plate with the dimension of 10mm X 10mm. The chemical composition of weld metal is listed in table 1. The weld joints were fabricated by continuous current and pulsed current gas tungsten arc welding mode. The joints were fabricated with and without filler wire. The different filler wires ERNiCrMo-4, ERNiCrMo-10 and ERNiCrMo-14 are employed in the present study to fabricate the weld joints. The chemical composition of the filler wires also listed in table 2. The corrosion samples are polished with silicon carbide emery sheet up to 2000 grade and cleaned with acetone to remove dirt. The corrosion test samples are shown in figure 1.

Table 1 Chemical composition of Alloy 686 base metal and different filler wires. [19-21]

	Ni	Mo	Cr	Fe	W	Mn	C	P	S	Ti	Si	Co	Al	Cu	Vd
Inconel 686	59.725	15.83	19.88	0.858	3.21	0.31	0.01	0.008	0.17	0.005	0.076	-	-	-	-
ERNiCrMo - 4	57.1	16.1	16.1	5.9	3.3	0.5	0.01	0.01	0.001	-	0.02	0.4	-	0.15	0.15
ERNiCrMo -10	57.023	13.5	21.5	3.1	3	0.02	0.01	0.005	0.002	-	0.04	1.8	-	-	-
ERNiCrMo- 14	58.2	16.4	20.5	0.3	4	0.2	0.01	0.002	0.001	0.04	0.06	-	0.3	0.01	-

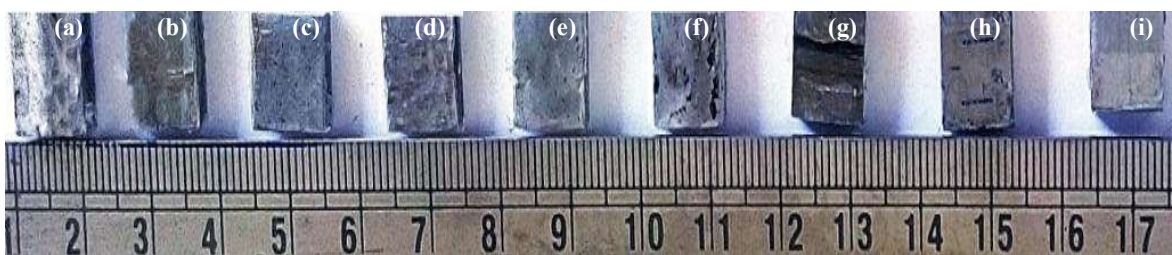


Figure 1 Weldment of corrosion test samples (a) GTAW Autogenous (b) PCGTAW Autogenous (c) GTAW- ERNiCrMo-4(d) PCGTAW- ERNiCrMo-4 (e) GTAW- ERNiCrMo-10 (f) PCGTAW- ERNiCrMo-10 (g) GTAW- ERNiCrMo-14 (h) PCGTAW- ERNiCrMo-14 (i) Base Metal

## 2.2 Electrochemical measurements

The Potentiodynamic corrosion studies on the weldments and base metal of alloy 686 were carried out with the help of electrochemical corrosion analyzer (Make: CH instruments). The computerized experimental setup is shown in figure 2. The cap surface of the weldment was utilized for corrosion study & exposed area is about 1 cm<sup>2</sup>, remaining area was covered with insulation tape. Synthetic sea water environment is prepared as per standard of ASTM D1141-2013 [22] and chemical composition of the solution is listed in the table 2. The corrosion rate was evaluated by Potentiodynamic Polarization testing as per ASTM G59-97(2014) [23]. In this method three electrodes namely; working electrode (1 cm<sup>2</sup> exposure area of the test sample), Counter electrode (platinum wire) and a Reference electrode (SCE passing through luggin capillary probe) were used to perform the electrochemical testing. To diminish the IR drop (potential drop due to solution resistance), the working electrode and luggin capillary were kept as close as possible. Before each electrochemical measurement, the access of steady state open circuit potential (OCP) can be made possible by immersing the working electrode for 20 minutes in corrosive solution. The detailed corrosion rate of alloy 686 weldments can be obtained by Tafel Polarization plots, and it also furnishes relevant electrochemical kinetic parameters details like corrosion rate. To plot this curve, the parameter considered are the electrode potential that is too changing the cathodic to the anodic direction ( $OCP \pm 200$  mV) along with the scan rate 1 mV s<sup>-1</sup>. The corrosion potential ( $E_{corr}$ ) and corrosion current ( $I_{corr}$ ), cathodic and anodic curves are shown in figure 6. By Tafel's methodology, the corrosion analysis is made, and the corrosion rate was calculated in mils per year, for each sample and values are listed in table 3.



**Figure 2. Computerized electrochemical corrosion analyzer**

**Table 2 Chemical composition of synthetic seawater\***

Compound	Concentration (g/L)
NaCl	24.53
MgCl <sub>2</sub>	5.2
Na <sub>2</sub> SO <sub>4</sub>	4.09
CaCl <sub>2</sub>	1.16
KCl	0.695
NaHCO <sub>3</sub>	0.201
KBr	0.101
H <sub>3</sub> BO <sub>3</sub>	0.027
SrCl <sub>2</sub>	0.025
NaF	0.003

\*After adjustment with 0.1 N NaOH the pH value = 8.2

### 3. Results & Discussion

#### 3.1. Microstructure Examination

Fig 3. (i) represents the microstructure of fusion zone center of alloy 686 weld joint fabricated by GTA welding process. Fusion zone consists of columnar dendrite and cellular structure. In contrast to GTAW, PCGTAW shows fine Equiaxed dendrite structure which is shown in figure 3.(ii). Figure 3. (iii) represents the fusion zone microstructure of alloy 686 weld joint produced by GTA welding process with filler wire ERNiCrMo-4. Fusion zone consists of columnar dendrite. But in PCGTAW the microstructure contains fine and equiaxed dendrite structure is shown in figure 3. (iv).

Figure 3. (v) illustrates the microstructure of fusion zone of alloy 686 weld joint fabricated with filler wire ERNiCrMo-10 by using GTA welding process. The fusion zone microstructure consists of cellular structure. In contrast to GTAW, PCGTAW shows Equiaxed dendrite microstructure which is shown in figure (vi).

Fig 3. (vii) shows the microstructure of fusion zone center of alloy 686 weld joint fabricated by GTA welding process. Fusion zone consists of columnar dendrite and cellular structure. In contrast to GTAW, PCGTAW is with fine equiaxed dendrite structure which is shown in figure (viii).

The fusion zone microstructure of all the four GTAW welded samples contain coarser grains with cellular structure at weld center and columnar dendrite structure at near to fusion boundary. This is due to steep thermal gradient at weld center than boundary. Coarse grains always decrease the corrosion resistance [24]. By contrast to GTAW, in PCGTAW the microstructures were fine and equiaxed grains. This is because of multiple instantaneous cooling rates available during PCGTAW welding. These superior cooling rates support the fine and much favorable microstructure formation. Here the solidification takes place much faster than GTAW and restrict the diffusion of alloying elements. PCGTAW microstructures are proof for refinement of grains and appreciate the necessity to switchover from GTAW to PCGTAW.

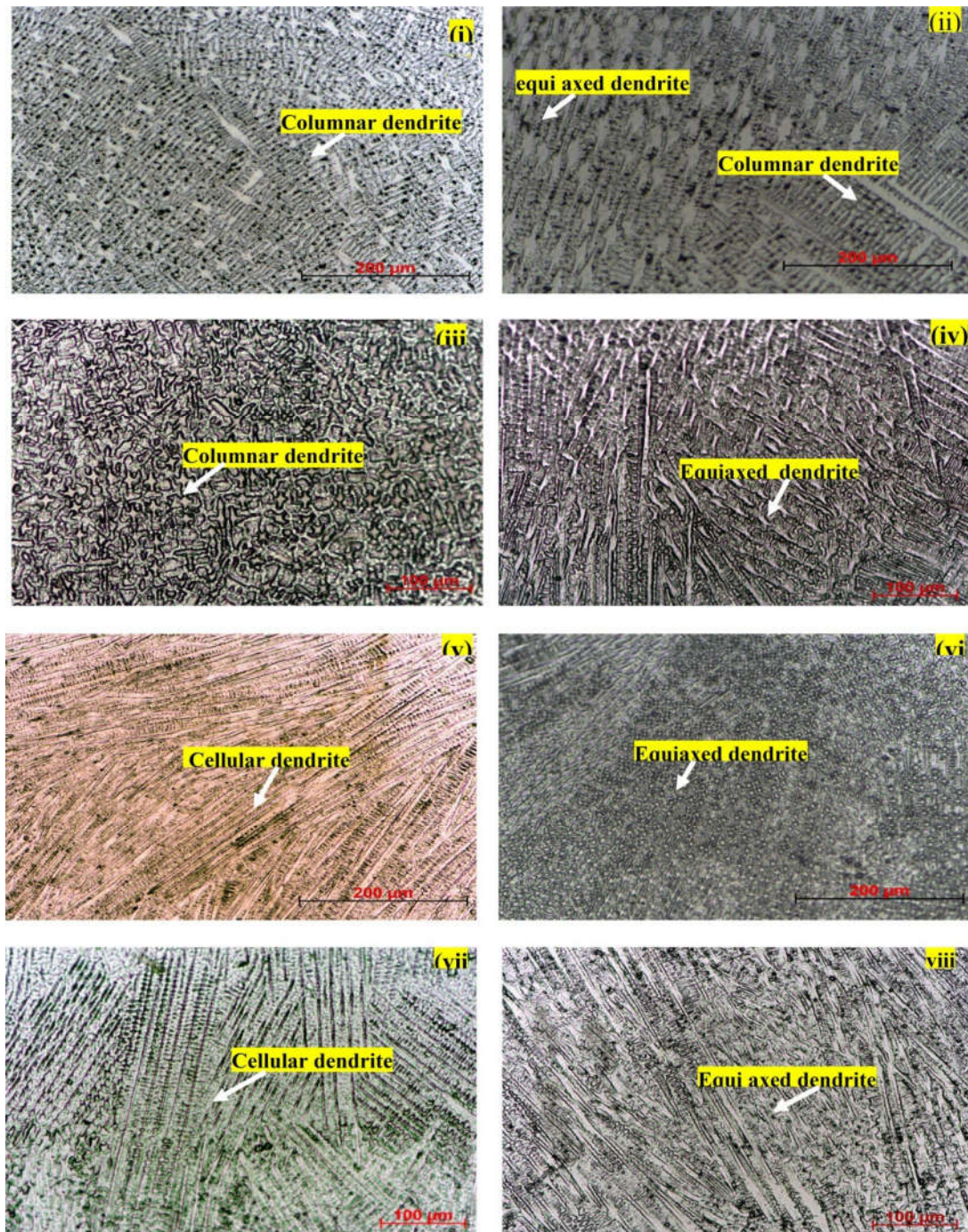


Figure 3. Weld center microstructures of Inconel alloy 686 weldments made by (i) GTAW – Autogenous (ii) PCGTAW – Autogenous (iii) GTAW – ERNiCrMo-4 (iv) PCGTAW – ERNiCrMo-10 (v) GTAW – ERNiCrMo-10 (vi) PCGTAW – ERNiCrMo-4 (vii) GTAW – ERNiCrMo-14 (viii) PCGTAW – ERNiCrMo-14

### 3.2. SEM/EDS Analysis

Figure 4a shows the high magnification scanning electron microscope (SEM) images of alloy 686 weldments made with GTAW-Autogenous mode. The alloying elements and their segregation in the fusion zone of Weldment are revealed by Energy Dispersive X-ray Spectroscopy (EDS) and it is

represented in Figure 4(i). The effect of microsegregation of alloying elements (Ni,Cr,Mo & W) in the interdendritic region of fusion zone weld center is only evaluated in this EDS examination. It is noted that the interdendritic region is enriched with Mo and diminished in Ni, Cr and W compared to dendrite core.

Figure 4b & 4(ii) represents the SEM/EDS analysis in the fusion zone of alloy 686 weldment fabricated by PCGTAW with Autogenous mode. It is clearly noted that there is less microsegregation in the interdendritic region of PCGTAW then compared with GTAW mode.

Figure 4c & 4(iii) illustrates the SEM/EDS examination of weld center of fusion zone of Weldment produced by GTAW using filler wire ERNiCrMo-10. As like GTAW Autogeneous mode, here also the interdendritic is enriched with Mo which leads to formation of secondary brittle phases.

Figure 4d & 4 (iv) shows the SEM/EDS analysis in the fusion zone of alloy 686 weldment fabricated by PCGTAW using filler wire ERNiCrMo-10. The EDS results explained that very minimum segregation is present in the interdendritic region.

Figure 5a & 5(i) demonstrates the SEM/EDS examination of alloy 686 weldment fabricated by GTAW with ERNiCrMo-4 filler wire. Here the Mo enriched segregation is very high than other weld joint joints.

Figure 5b & 5(ii) represents the SEM/EDS analysis in the fusion zone of alloy 686 weldment fabricated by PCGTAW with ERNiCrMo-4 filler wire. It is clearly noted that there is a bit higher microsegregation in the interdendritic region of PCGTAW when compared with other PCGTAW welded joints.

Figure 5c & 5(iii) illustrates the SEM/EDS examination of weld center of fusion zone of Weldment produced by GTAW using filler wire ERNiCrMo-14. As like other GTAW weldments, here also the interdendritic is enriched with Mo which leads to formation of secondary brittle phases.

Figure 5d & 5 (iv) shows the SEM/EDS analysis in the fusion zone of alloy 686 weldment fabricated by PCGTAW using filler wire ERNiCrMo-14. The EDS results elucidate that moderate segregation is present in the interdendritic region.

From above analysis it is clearly understandable that, in GTAW weldments, the microsegregation is significantly high when compared with PCGTAW. This is due to continuous heat input, high diffusion rate and minimum cooling potential. These factors raise possibility of more secondary phase's formation in GTAW weldments. It will end up with removal of Mo from stable Ni matrix and segregated at interdendritic region. Finally corrosion resistance is decreased in the welded specimens.

The SEM/EDS images of PCGTAW confirm that there is a lesser amount of microsegregation in their weldments. This is due to controlling of heat input through pulse variation of current. It offers variation in temperature cycle, enhancement in cooling rate, enhanced fluid flow and reduction of thermal gradient in the fusion zone weld pool. As a result, in a PCGTAW process, stable austenite matrix is maintained with uniform alloying elements, there is an improvement in corrosion resistance. Anyhow, corrosion resistance value is less, when compared with base metal.

Both Scanning Election microscope and optical electron microscope images proves that a better grain refinement is possible when switchover from GTAW to PCGTAW.

### 3.3. Electrochemical measurements:

Tafel polarization curves plotted for Weldment samples which were made by continuous and pulsed current GTA technique immersed in synthetic sea water environment is shown in Fig. (5)

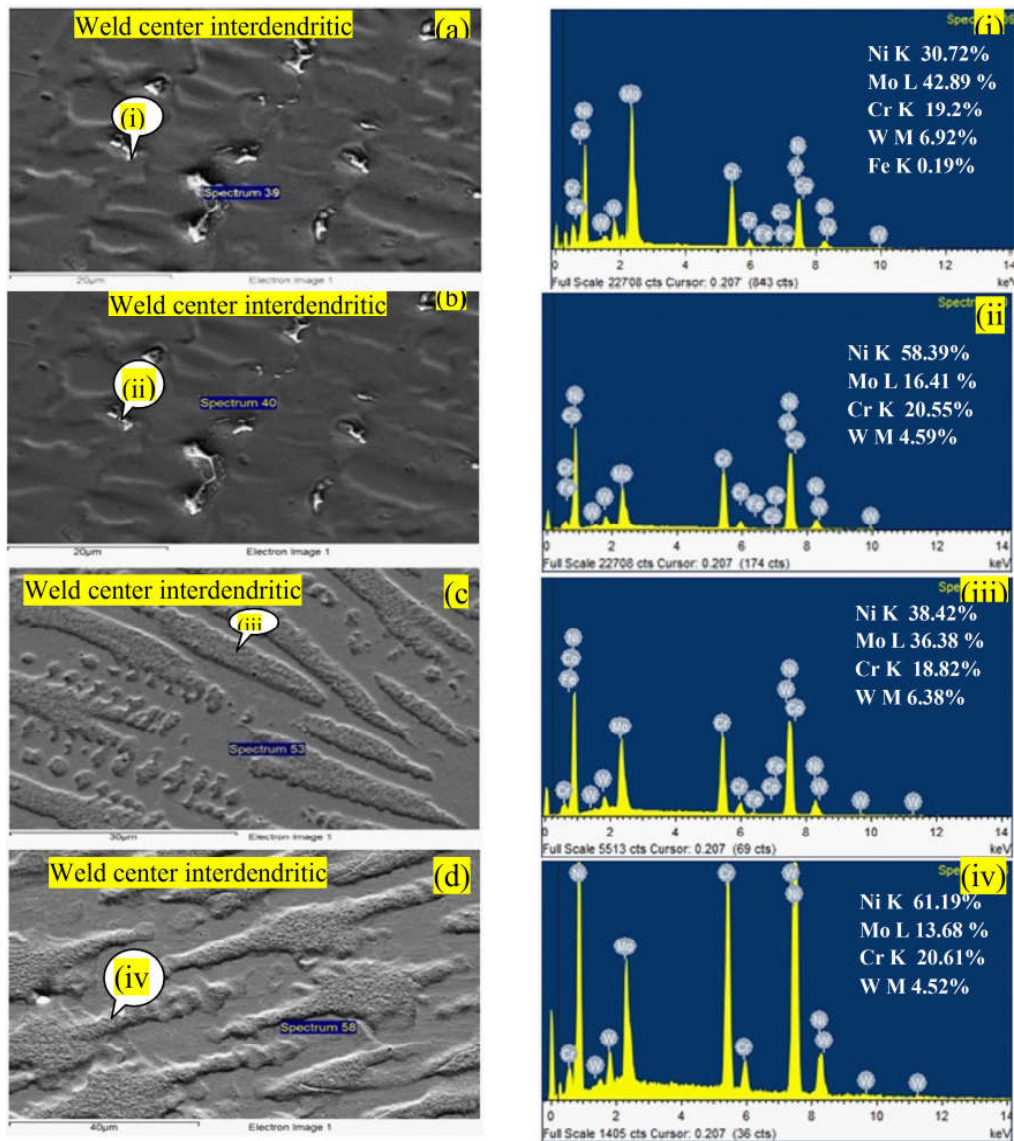


Figure 4 SEM images of weld center interdendritic region of a) GTAW Autogenous b) PCGTAW Autogenous c) GTAW filler wire with ERNiCrMo-10 d) PCGTAW filler wire with ERNiCrMo-10; EDS analysis of weld center interdendritic zone of i) GTAW Autogenous ii) PCGTAW Autogenous iii) GTAW filler wire with ERNiCrMo-10 iv) PCGTAW filler wire with ERNiCrMo-10

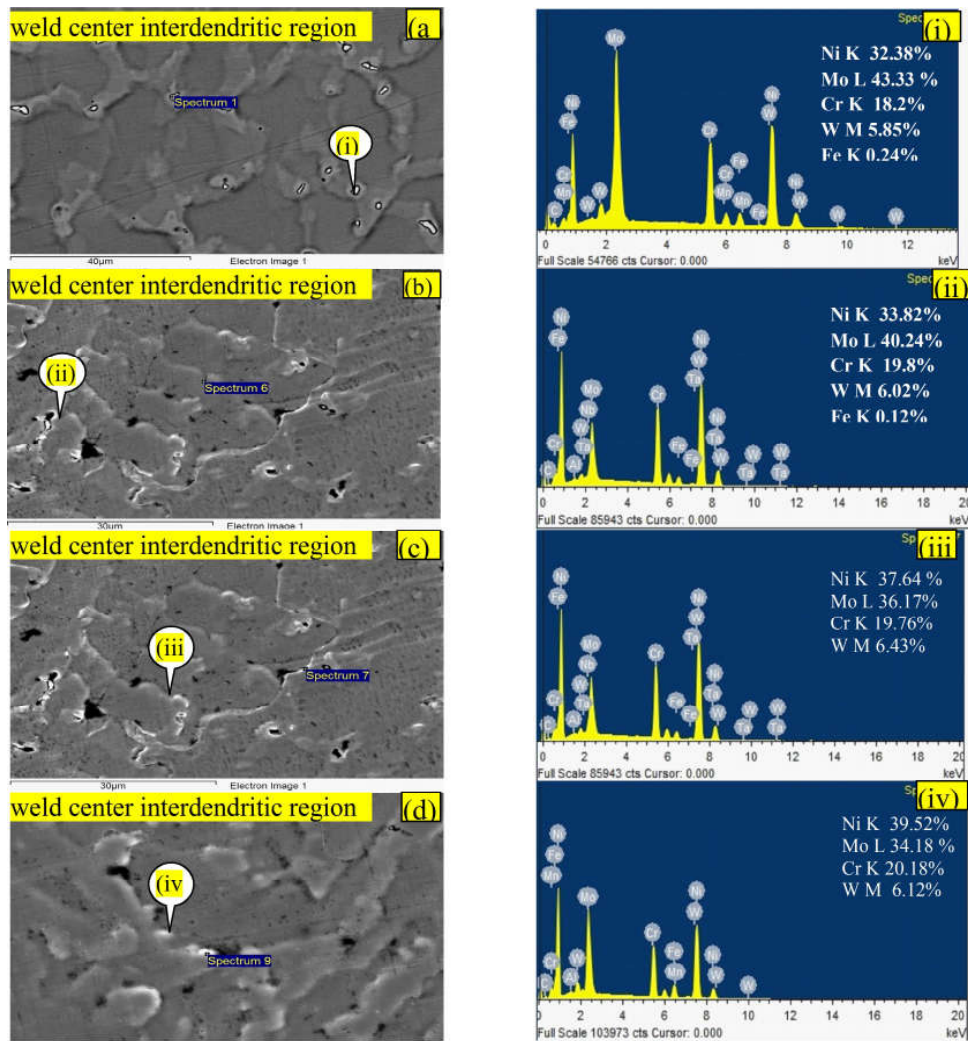


Figure 5 SEM images of weld center interdendritic region of a) GTAW with ERNiCrMo-4 filler wire b) PCGTAW with ERNiCrMo-4 filler wire c) GTAW with ERNiCrMo-14 filler wire d) PCGTAW with ERNiCrMo-14 filler wire; EDS analysis of weld center interdendritic zone of i) GTAW ERNiCrMo-4 ii) PCGTAW ERNiCrMo-4 iii) GTAW ERNiCrMo-14 iv) PCGTAW ERNiCrMo-14

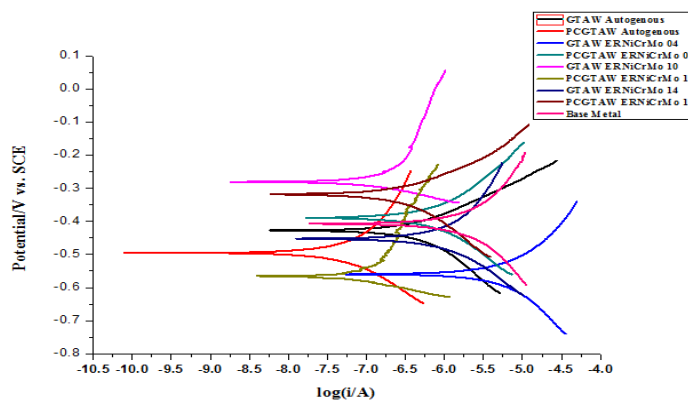


Figure 6 Tafel polarization curves of alloy 686 Weldments immerse in synthetic sea water

Table 3 corrosion rate of Base metal and different weld samples

Weldment type	Corrosion rate (mpy)
Base Metal	0.01
GTAW - Autogenous	0.5
PCGTAW - Autogenous	0.06
GTAW – ERNiCrMo-4	2.83
PCGTAW - ERNiCrMo-4	0.78
GTAW - ERNiCrMo-10	0.16
PCGTAW - ERNiCrMo-14	0.11
GTAW - ERNiCrMo-14	1.02
PCGTAW - ERNiCrMo-14	0.28

The base metal has the least corrosion rate of 0.01 mpy and its value almost match with available literature [3]. From Table 3, it is clear that the corrosion resistance of the weldment sample fabricated by PCGTAW process is higher as compared to the conventional GTAW mode. Arulmurugan et al.[13] reported that same when moving from GTAW to PCGTAW; Weldments are with finer & equiaxed grain microstructure, reduction in microsegregation and betterment in properties. Balasubramanian et al. [24] is also stated that if the grain size is small and finer, there will be an enhancement in corrosion resistance. From the table 3 it is clear that GTAW with filler wire ERNiCrMo-4 has shows the highest corrosion rate (2.04 mpy) because of the possibility of more microsegregation of secondary phases at interdendritic regions. Since alloy 686 is having more than 15% Mo content, there is a possibility of formation of secondary phases which are undesirable and causes premature failures in weldments [4]. The reason for high corrosion rate in that particular filler wire is, it is not a matching composition with base metal. Manikandan et al. [25] also reported the same in their studies on alloy C-276, by using mismatch filler wire with base metal will lead to severe microsegregation and properties reduction.

#### 4. Conclusion

This research work has provided a comparison of the corrosion behavior in terms of corrosion rate for the alloy 686 Weld joints made by conventional GTA process and pulsed mode of GTA process. From the experimental examination, the conclusions made were mentioned below,

1. Weld joints produced with GTAW both in autogenous and with three different filler wires, show comparatively coarse microstructure with columnar and cellular grains in their fusion zone. While welds fabricated with PCGTAW show relatively finer microstructure with equiaxed grains
2. SEM/EDS analysis reveals that PCGTAW Weldment's fusion zone were freedom from secondary brittle phases. In contrast, GTAW process weld joints were having higher segregation in their fusion zone.
3. The corrosion rates of the weldment tested under normal 0.1% NaCl conditions can be arranged in the Order PCGTAW – Autogenous > PCGTAW – ERNiCrMo-10 > GTAW – ERNiCrMo-10 > PCGTAW – ERNiCrMo-14 > GTAW – Autogenous > PCGTAW – ERNiCrMo-4 > GTAW – ERNiCrMo-14 > GTAW – ERNiCrMo-4. Weld samples made with PCGTAW process have posses less corrosion rate, i.e., more corrosion resistance than GTAW weldments.
4. The highest corrosion rate is on GTAW– ERNiCrMo-4, because of more microsegregation at interdendritic region due to the mismatch between filler material and base metal.
5. PCGTAW weldment fabricated by Autogenous mode had the excellent corrosion resistance than other weldments, because of finer grains with equiaxed microstructure and reduced microsegregation.

## References

- [1] Anselmo N, May J E, Mariano N A, Nascente P A P and Kuri S E 2006 *J. Mater. Sci. Eng., A*. **A 428** 73
- [2] webdata: [http://www.ironhaven.nl/isa/Corrodium\\_marine.pdf](http://www.ironhaven.nl/isa/Corrodium_marine.pdf)
- [3] webdata: <http://www.specialmetalswiggins.co.uk/pdfs/products/INCONEL%20alloy%20686.pdf>
- [4] John Dupoint N, John Lippold Cand and Samuel Kiser D 1999 *Welding Metallurgy and Weldability of Nickel-Base alloys*. (New Jersey: John Wiley & Sons) 49-51
- [5] Hayes J R, Gray J J, Szmodis A W and Orme C A 2006 *Proc. Int. conf. on NACE Corrosion science section*. **6** 62 491
- [6] Raúl B. Rebak and Paul Crook 2004 *Proc. Int. Conf. on American Society of Mechanical Engineers Pressure Vessels and Piping Division* (San Diego) , p 1-8, UCRL-PROC-203671
- [7] Craig B D and McClymonds L A 1981 *Proc. Int. Conf. on National Association of Corrosion Engineers Vol. 37-8* p485
- [8] webdata: Special Metals Lewis E Shoemaker and James R Crum [http://www.pccforgedproducts.com/web/user\\_content/files/wyman/Corrosion%20Performance%20and%20Fabricability%20of%20the%20New%20Generation%20of%20Highly%20Corrosion%20Resistant%20NiCrMo%20Alloys.pdf](http://www.pccforgedproducts.com/web/user_content/files/wyman/Corrosion%20Performance%20and%20Fabricability%20of%20the%20New%20Generation%20of%20Highly%20Corrosion%20Resistant%20NiCrMo%20Alloys.pdf)
- [9] Guangyi M A, Dongjiang W U and Dongming G U O 2011 *J. Metall. Mater. Trans. A*. **42A** 3853
- [10] Manikandan M, Hari P R, Vishnu G, Arivarasu M, Devendranath Ramkumar K, Arivazhagan N, Nageswara Rao M and Reddy G M 2014 *J. Procedia Mater. Sci.* **5** 2233
- [11] Radhakrishna CH, Prasad Rao K, and Srinivas S 1995 *J. Mater. Sci. Lett.*, **14** 1810
- [12] Janaki Ram G D, Venugopal Reddy A, Prasad Rao K and Madhusudhan Reddy G 2004 *J. Sci. Technol. Weld. Joining* **9(5)** 390
- [13] Manikandan M, Arivazhagan N, Nageswara Rao M and Reddy G M 2015 *J. Acta Metall. Sin. (Engl. Lett.)* **28(2)** 208
- [14] Manikandan M, Arivazhagan N, Arivarasu M, Mageshkumar K, Deva N. Rajan, Arulmurugan B, Prasanth P, Sukumar S and Vimalanathan R 2017 *J. Trans Indian Inst Met.* DOI 10.1007/s12666-017-1045-6
- [15] Arulmurugan B and Manikandan M 2017 *J. Mater. Sci. Eng., A.*, **A691** 126
- [16] Stern M and Geary A L 1957 *J. Electrochem. Soc.* **104** 56
- [17] Sergio Luiz de Assis, Stephan Wolyne and Isolda Costa 2006 *J. Electrochim. Acta* **51** 1815
- [18] Zhang X L, Jiang Zh H , Yao Zh P, Song Y and Wu Zh.D. 2009 *J. Corros. Sci.* **51** 581
- [19] webdata: <http://www.pinnaclealloys.com/wp/wp-content/uploads/2015/11/Pinnacle-Alloys-ERNiCrMo-4-C-276.pdf>
- [20] webdata: <http://www.pinnaclealloys.com/wp/wp-content/uploads/2015/11/Pinnacle-Alloys-ERNiCrMo-10-622.pdf>
- [21] webdata: <https://www.weldingwarehouseinc.com/products/aws/a5-14/ernicrmo-14/>
- [22] ASTM D1141 – 98 (2013), Standard Practice for the Preparation of Substitute Ocean Water, ASTM International.
- [23] ASTM G59-97(2014), Standard Practice for the conduction of Potentiodynamic Polarization Resistance test, ASTM International.
- [24] Balasubramanian M, Jayabalan.V and Balasubramanian V 2008 *J.Mater..Des.* **29** 1359
- [25] Manikandan M, Arivazhagan N, Nageswara Rao M and Reddy G M 2014 *J. Manuf. Processes* , **16** 563